PROCEEDINGS OF SCIENCE

Unveiling the X-ray broad band continuum and iron line complex in Mkn 841

P.O. Petrucci[*1], **G. Ponti**[2], **G. Matt**[2], **A. Longinotti**[3], **M. Mouchet**[4], **C. Boisson**[4], **L. Maraschi**[2], **J. Malzac**[6], **K. Nandra**[7], **P. Ferrando**[8]

[1] *LAOG, Grenoble, France,* [2] *Università degli Studi "Roma tre", Roma, Italy ,* [3]*VILSPA/ESA, Madrid, Spain,* [4]*LUTH, Obs. Paris/Meudon, France,* [5]*OAB, Milano, Italy,* [6]*CESR, Toulouse, France,* [7] *Imperial College, London, UK,* [8] *DAPNIA/CEA, Saclay, France*
E-mail: pierre-olivier.petrucci@obs.ujf-grenoble.fr

Mkn 841 has been observed during 3 different periods (January 2001, January 2005 and July 2005) by XMM-Newton for a total cumulated exposure time of 108 ks. We present in this paper a broad band spectral analysis of the complete EPIC-pn data sets. These observations confirm the presence of the strong soft excess and complex iron line profile known to be present in this source since a long time. They also reveal their extreme and puzzling spectral and temporal behaviors. Indeed, the 0.5-2 keV soft X-ray flux decreases by a factor 3 between 2001 and 2005 and the line shape appears to be a mixed of broad and narrow components, both variable but on different timescales. The broad-band 0.5-10 keV spectra are well described by a model including a primary power law continuum, a blurred photoionized reflection and a narrow iron line, the blurred reflection fitting self-consistently the soft excess and the broad line component. The origin and nature of the narrow component is unclear.

VI Microquasar Workshop: Microquasars and Beyond
September 18-22 2006
Società del Casino, Como, Italy

[*] Speaker.

PoS(MQW6)089

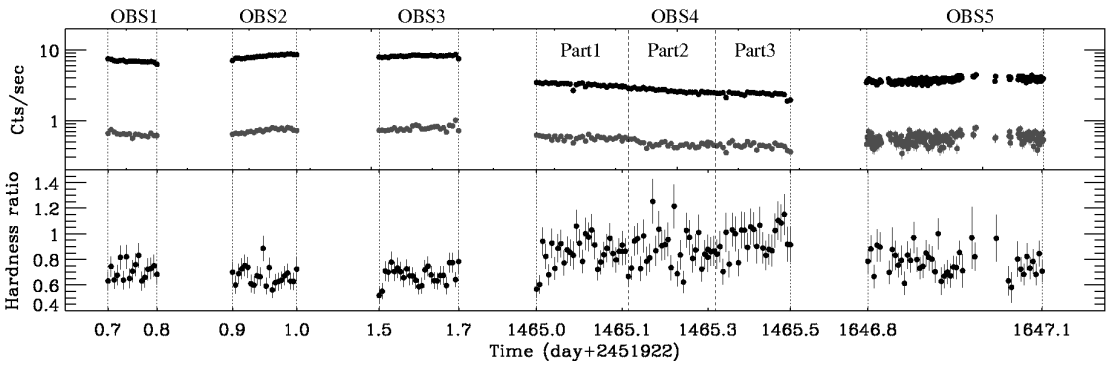

Figure 1: Top: 0.5-10 keV (upper points) and 3-10 keV (lower points) count rate light curve. Bottom: Hardness ratio (5-10 keV)/(3-5 keV) light curve.

1. The data

Mkn 841 has been observed 5 times by XMM-Newton. We focus here on the Epic-pn data only. The date and exposure time of the different observations are summarized in Table 1. For the spectral analysis we have divided OBS4 in 3 parts (noted part1, part2 and part3 in the following) of about 15 ks each.

Obs	Date	Exposure ks	3-10 keV flux 10^{-11} erg.s^{-1}cm^{-2}
1	13 Jan. 2001	8.5	1.05
2	13 Jan. 2001	10.9	1.17
3	14 Jan. 2001	13.3	1.24
4	16 Jan. 2005	46.0	0.85
5	17 Jul. 2005	29.1	0.95

Table 1: The XMM-*Newton* observations log.

2. Light curves and hardness ratio

We have plotted on top of Fig. 1 the 0.5-10 keV EPIC-PN count rate light curves of the different XMM-*Newton* observations of Mkn 841 as well as the hardness ratio (5-10 keV)/(3-5 keV) at the bottom. The time binning is 500 sec. The 0.5-10 keV count rate decreases by a factor $\sim$4 in 4 years while the hardness ratio increases, reaching maximum values during OBS 4. The 3-10 keV count rate has been also plotted in Fig. 1. It shows variations of $\sim$ 60% implying that the 0.5-10 keV count rate variability is dominated by the soft ($<$ 3 keV) X-ray variability, at least on long time scale. Smooth soft *and* hard flux variabilities up to $\sim$50% are also visible on tens of ks.

3. Spectral analysis

3.1 Phenomenological analysis

The first step of the spectral analysis was to fit the 3-10 keV data with a simple power law. We clearly observed a strong soft excess below 2-3 keV and a fluorescent iron line complex near 6.4 keV. These spectral features are observed in all the other data sets. The second step was to include very simple spectral components to reproduce the observed features. We use a power law for the continuum and a gaussian for the iron line. We fit the data above 3 keV first. Then we fix the different parameters and include the data below 3 keV down to 0.5 keV and we add a simple black body component to model the soft excess. The best fits are clearly not satisfactory for all the observations (cf. Tab. 2). Large discrepancies are present especially below 3 keV, a black body being a poor approximation of the soft excess component. Anyway different remarks, weakly affected by the goodness of the fit, can already been done:

- The spectral variability appears to be due to both variable high energy (above 3 keV) continuum and variable soft excess. Indeed the photon index varies by ~ 0.5 between 2001 and 2005, while the soft X-ray flux, below 3 keV, decreases by a factor 3, i.e. more than the flux variability (of $\sim 60\%$) expected if the power law continuum was the only variable component.
- The photon index reaches values as small as 1.3 during OBS 4, unusually hard for a Seyfert X-ray spectrum.
- The best fit requires a narrow line in all the observation but OBS 3 and part 2 of OSB 4 where a broad component is found (cf. Tab. 2). The apparent variability of the line in 2001 was already noted by [4] and [3] and we observe the same variability behavior during the 2005 observations. This will be discussed in more details in the next section.

3.2 Line variability

The line variability is clearly visible on the map excess reported in Fig. 2 (and produced following the method describe in [2]). this figure shows that the line complex (i.e. line+continuum) is variable on timescale as short as $\sim$10 ks. We have also plotted the contour plots, at 68 and 90 % confidence level, of the line flux vs. line width for the different observations on Fig. 3.

The interpretation by [3] of the line variability observed in 2001 invoked local illumination by a flare inducing an hotspot in the inner disc, which then becomes progressively broadened as the disc rotates. This would explain the observed changes of the line width. The line variability behaviour in Jan. 2005 looks very similar to the one observed in 2001 (i.e. variation of the line width) but somes differences still exist . First of all, we note an increase of the line flux during part 2, a factor 2-3 larger than in part 1 and 3 while in 2001 the line flux is consistent with being constant (cf. Fig. 3a). More importantly we detect some residuals of a narrow component near 6.4 keV in part 2 of OBS 4. There are also some residuals near 5-6 keV in part 1 and 3 suggesting the presence of a broad component. To check this, we have added a second gaussian to the model. A narrow component is indeed detected in part 2 while broad ones are found in part 1 and 3. The addition of this second line is significant at more than 99.7%, 93% and 98.9% (following the F test) for part

Obs	N_H	Γ	E_{FeK_α}	σ_{FeK_α}	F_{FeK_α}	EW	kT_{bb}	χ^2/dof
	10^{-2}		keV	10^{-5}	eV	keV		
1	<2.4	$1.81^{+0.07}_{-0.09}$	$6.25^{+0.15}_{-0.14}$	<2.4	$1.4^{+3.2}_{-0.6}$	90^{+210}_{-35}	$0.20^{+0.01}_{-0.01}$	548/244
2	<2.4	$1.91^{+0.06}_{-0.08}$	$6.39^{+0.06}_{-0.05}$	<0.2	$2.7^{+1.0}_{-0.8}$	170^{+60}_{-50}	$0.18^{+0.01}_{-0.01}$	510/263
3	<2.4	$1.91^{+1.00}_{-0.08}$	$6.57^{+0.38}_{-0.46}$	$0.8^{+1.2}_{-0.4}$	$4.0^{+152.0}_{-1.8}$	244^{+9200}_{-110}	$0.17^{+0.01}_{-0.01}$	397/263
4 part 1	<3.3	$1.43^{+0.05}_{-0.07}$	$6.44^{+0.05}_{-0.04}$	<0.9	$1.3^{+2.5}_{-0.5}$	90^{+170}_{-40}	$0.13^{+0.01}_{-0.01}$	334/273
4 part 2	<2.6	$1.42^{+0.09}_{-0.04}$	$5.50^{+0.52}_{-0.43}$	$1.0^{+2.1}_{-0.5}$	$5.9^{+25.5}_{-4.1}$	420^{+1800}_{-290}	$0.14^{+0.01}_{-0.01}$	342/266
4 part 3	<2.6	$1.30^{+0.07}_{-0.06}$	$6.51^{+0.03}_{-0.03}$	<0.1	$1.6^{+2.1}_{-0.4}$	140^{+80}_{-40}	$0.14^{+0.01}_{-0.01}$	367/266
5	<2.6	$1.65^{+0.05}_{-0.06}$	$6.49^{+0.09}_{-0.07}$	<0.25	$1.9^{+0.5}_{-0.8}$	140^{+40}_{-60}	$0.12^{+0.01}_{-0.01}$	389/281

Table 2: Best fit values obtained with a simple model including a power law for the continuum, a gaussian for the iron line and a black body for the soft excess.

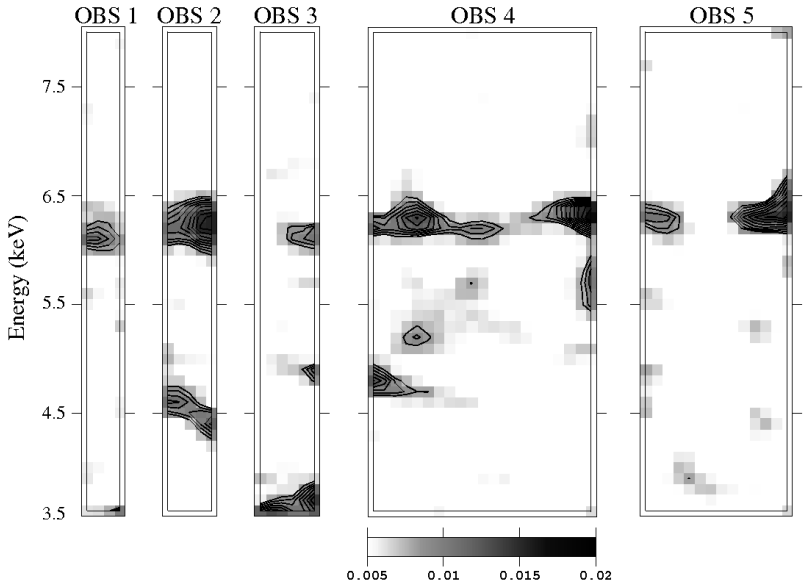

Figure 2: Map excess for the different observations.

1, 2 and 3 respectively. It is also worth noting that the narrow line detected in part 2 has a weak flux but still in good agreement with the fluxes of the other narrow components detected in OBS 1, in 2001, in part 1 and 3 of OBS 4 and in OBS 5. However it is smaller by a factor 3-4 than the flux of the narrow line observed in OBS 2. The corresponding contour plot has been over-plotted on Fig. 3b. Concerning the broad component detected in part 1 and 3, they are consistent with each other and with the broad component of part 2. Thus the line complex during OBS 4 appears to be a mix of broad and narrow components. This contrasts with what we observed in the other observations (OBS 1, 2 or 3 and OBS 5) where the addition of a second gaussian line in does not improve significantly the fits.

We have also tried to fit the 3 parts of OBS 4 with a model of line emission from a relativistic accretion disk (DISKLINE model of XSPEC) fixing the accretion disc outer radius to 1000 r_g and

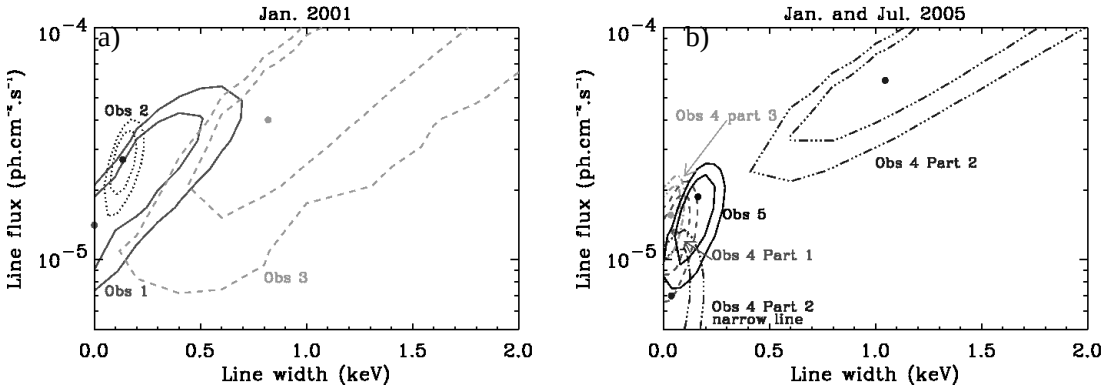

Figure 3: Contour plots (68 and 90 %) of the line width vs. line flux obtained when fitting the 3 observations of Jan 2001 (left) and observations of Jan. 2005 and Jul. 2005 (right). In all cases, the model includes a simple power law + gaussian line. We have also over plotted on the right the contour plot of the narrow component detected in part 2 of OBS 4.

keeping the inclination angle constant between the different spectra. The fit is good, with a best fit inclination angle of 47^{+5}_{-8} degrees. We can note however that the fit with two gaussians is slightly better for part 3 of OBS 4 compared to the DISKLINE one (χ^2/dof=131/140 compared to 141/141) thanks to a better fit of the narrow component.

4. A more physical analysis: blurred ionized reflection?

Recent studies suggest that an appealing explanation for the presence of strong soft excesses in AGNs could be blurred (photoionized) reflection from the accretion disc [1]. These authors already applied this model to the OBS 3 of Mkn 841 with success. Moreover, in the cases in which a broad Fe line is clearly detected (such as in MCG–6-30-15) the model is very robust because the soft excess and broad Fe line are fitted self–consistently with the same relativistically blurred reflection model. The characteristics of the line complex in Mkn 841, with the presence of a variable broad line component well fitted by a blurred (DISKLINE) profile, and a strong soft excess, suggest that photoionized reflection may play also an important role in this source. To test these assumptions we have used a more physical model with the following components: 1) a neutral absorption 2) a cut-off power law continuum (the high energy cut-off being fixed to 300 keV), 3) a blurred photoionized reflection and 4) a narrow line component if needed. For the blurred reflection, we use the tables of the Ross & Fabian code [5] convolved with a Laor profile (kdblur kernel). This component reproduces the soft excess and the broad iron line.

We obtain very good fits in most of the cases, with some problems with OBS 5 where important absorption features are present at low energy. The corresponding best fit parameter values are reported in Tab. 3 and the data and ratios of OBS 4 part 3 is plotted on Fig. 4. This model depends strongly on the emissivity law index q ($j \propto r^{-q}$) and the inner disc radius r_{in}. Roughly speaking, r_{in} controls the maximal relativistic blurring effect while q controls the relative importance of these effects on the total line profile. Thus the fit of the broad line component as well as the soft excess requires a fine tuning of these two parameters. For example, large q and small r_{in} imply strong

Obs.	Γ	ξ	q	r_{in} r_g	χ^2/dof
1	$2.31^{+0.07}_{-0.09}$	190^{+160}_{-80}	$8.7^{+1.3}_{-1.4}$	$1.3^{+0.2}_{-0.1}$	248/241
2	$2.28^{+0.10}_{-0.05}$	117^{+140}_{-10}	$8.2^{+1.6}_{-1.2}$	$1.4^{+0.1}_{-0.2}$	227/260
3	$2.19^{+0.08}_{-0.04}$	54^{+54}_{-12}	$5.3^{+3.1}_{-0.7}$	$1.4^{+0.2}_{-0.2}$	292/273
4-1	$1.50^{+0.10}_{-0.02}$	200^{+10}_{-20}	$6.4^{+0.6}_{-0.5}$	$1.8^{+0.2}_{-0.6}$	283/269
4-2	$1.57^{+0.05}_{-0.04}$	140^{+2}_{-7}	$6.0^{+0.3}_{-0.3}$	$1.7^{+0.1}_{-0.1}$	292/264
4-3	$1.49^{+0.02}_{-0.04}$	140^{+60}_{-10}	$7.0^{+1.1}_{-0.7}$	$2.1^{+0.1}_{-0.2}$	283/264
5	$1.63^{+0.01}_{-0.02}$	300^{+10}_{-40}	$7.0^{+1.2}_{-0.6}$	$2.0^{+0.2}_{-0.1}$	371/278

Table 3: Best fit results obtained with the blurred ionized reflection model. ξ= ionization parameter, q=disc emissivity law index, r_{in}= disc inner radius. The addition of a warm absorber in OBS 5 highly improves the fit ($\Delta\chi^2$=80)

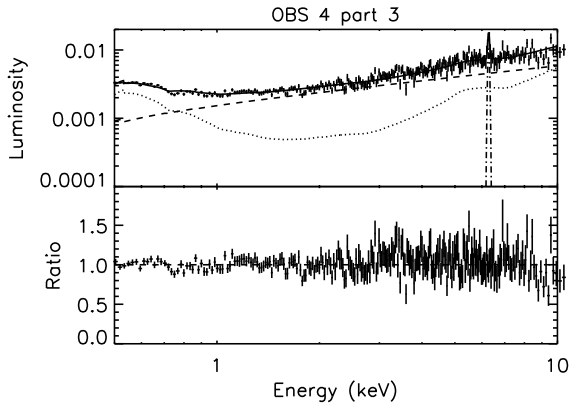

Figure 4: Best fits of OBS 4 part 3 obtained with the blurred ionized reflection. On top is reported the unfolded best fit model (solid line) with the different spectral components: cut-off power law (dashed line), blurred ionized reflection (dotted line) and the narrow gaussian line (dot-dashed line). At the bottom we have plotted the corresponding data/model

relativistic effects that completely smeared out the lines. This is indeed what we find in the case of OBS 1, OBS 2 and OBS 5 where no broad line is detected. On the other hand, for a given r_{in}, smaller q reduces the importance of the relativistic blurring effects and the broad line is more easily detectable like in OBS 3 and OBS 4. The smaller values of q are obtained for OBS 3 and part 2 of OBS 4 where the stronger broad lines are detected. We note that the best fits obtained for the 2001 observations also agree with simultaneous BeppoSAX (2-200 keV) data which is quite encouraging. It is worth noting however that in almost all cases but OBS 3 the addition of a narrow line is required by the data. This is due to the large blurring effects needed to fit the soft excess that smeared out the iron line and then prevent a good fit of the narrow component. Thus, if the blurred ionized reflection model looks very promising in explaining the soft excess and broad line component behaviors in Mkn 841, the origin of the narrow component, which appears variable on relatively short time scale, at least in 2001, is still unclear.

References

[1] J. Crummy, A. C. Fabian, W. N. Brandt, and T. Boller, *Investigating ionized disc models of the variable narrow-line Seyfert 1 PG 1404+226*, MNRAS **361**, 1197–1202 (2005) [astro-ph/0506119].

[2] K. Iwasawa, G. Miniutti, and A. C. Fabian, *Flux and energy modulation of redshifted iron emission in NGC 3516: implications for the black hole mass*, MNRAS **355**, 1073–1079 (2004).

[3] A. L. Longinotti, K. Nandra, P. O. Petrucci, and P. M. O'Neill, *On the variability of the iron Kα line in Mrk 841*, MNRAS **355**, 929–934 (2004).

[4] P. O. Petrucci, G. Henri, L. Maraschi, P. Ferrando, G. Matt, M. Mouchet, C. Perola, S. Collin, A. M. Dumont, F. Haardt, and L. Koch-Miramond, *A rapidly variable narrow X-ray iron line in Mkn 841*, A&A **388**, L5–L8 (2002).

[5] R. R. Ross and A. C. Fabian, *A comprehensive range of X-ray ionized-reflection models*, MNRAS **358**, 211–216 (2005) [astro-ph/0501116].